Delayed γ Rays between 2 and 80 μsec after U^{235} (n, f) and Pu^{239} (n, f)*

R. B. WALTON† AND R. E. SUND
Gulf General Atomic Incorporated, San Diego, California 92112

(Received 3 September 1968)

Measurements of the energy spectrum of delayed γ rays from the neutron fission of Pu^{239} and U^{235} were performed with a NaI detector at a number of time intervals between 2 and 80 μsec. The data showed three new prominent γ rays with energies of 205, 390, and 1330 keV, two unresolved γ rays having energies of approximately 110 keV, and the six γ rays with energies of 260, 460, 720, 850, 910, and 1250 keV which were observed in previous studies for $t>50$ μsec after fission. Absolute intensities of the new γ rays were obtained using the normalization factor derived from the relative intensities of the last six γ rays and their previously determined absolute intensities. The 205-, 390-, and 1330-keV γ rays probably result from the cascade decay of a single isomer which has a half-life of 3.4 ± 0.4 μsec and fission yields of (1.30 ± 0.30) and $(0.63\pm0.20)\%$ per fission of Pu^{239} and U^{235}, respectively. Half-lives and yields were also obtained for the unresolved 110-keV photopeaks, but these results are tentative because of uncertainties in the data. The fission yields, cascade γ rays, and half-lives of the isomers responsible for early delayed γ rays from $U^{235}(n, f)$ and $Pu^{239}(n, f)$ are summarized, and total intensities and energy emission rates of γ rays with energies greater than 140 keV are presented as a function of time after fission over the range from 2 μsec to 25 msec.

1. INTRODUCTION

In recent years several measurements of delayed γ rays emitted at times less than 100 sec after fission have been performed. Fisher and Engle[1] obtained absolute energy spectra of γ rays as a function of time from 0.2 to 45 sec after the fast-neutron fission of Th^{232}, U^{233}, U^{235}, U^{238}, and Pu^{239}, and Maienschein *et al.*,[2] made similar measurements over the time range from 1 to 1800 sec after the fission of U^{235} by thermal neutrons. The γ-ray energy emission rates observed in the range from 0.2 to $\sim$10 sec have been successfully predicted by Griffin[3] with a model which describes the gross behavior of β decays of the initial fragments and subsequent emission of γ rays by the daughter nuclei. Maienschein *et al.*[2] also investigated γ rays emitted between 50 nsec and 1.4 μsec after $U^{235}(n, f)$ and found an intense component with an apparent half-life of about 100 nsec which they attributed to fission fragment isomers. In addition, results on delayed γ rays have been obtained by Johansson[4] for times less than $\sim$300 nsec after the spontaneous fission of Cf^{252} and by Popeko *et al.*[5] for the time range from 10 to 70 nsec after the thermal-neutron fission of U^{235}.

The work described in this paper is a continuation of research at Gulf General Atomic on the intensity and energy spectrum of γ rays versus time of emission after fission. Techniques utilizing pulsed beams of bremsstrahlung and neutrons from an electron LINAC have been developed for studies in the time region from a few μsec to $\sim$0.1 sec after fission, where no previous quantitative data existed. Our first study[6] consisted of measurements of the γ-ray intensity emitted between 100 μsec and 7 sec after the photofission of U^{238}, U^{235}, and Th^{232}. The intensities decreased with time in the region from 100 to 500 μsec with an effective half-life of $\sim$70 μsec, indicating that fission fragment isomers are the dominant source of γ rays in this time region. Between 1 msec and 0.1 sec, the observed γ-ray activities decreased little. The measured intensities in this "plateau" time region were in good agreement with the values derived from Griffin's theoretical work on γ rays which follow β decay of fission fragments.[3,6] Subsequently, we measured the energy spectra and relative intensities of delayed γ rays from the neutron fission of U^{235} and Pu^{239} as a function of time in the interval from 50 μsec to the plateau region.[7] Six prominent γ rays were observed in the spectra, and their intensities and half-lives indicated that they resulted from the decay of three isomers, each emitting a pair of γ rays in cascade. The results of this experiment were normalized in the plateau region to Griffin's calculated time-dependent intensities,[3] which fitted the experimental data of Fisher and Engle[1] for times greater than 0.2 sec after fission.

The purpose of the present experiment was to measure the intensities and energy spectra of delayed γ rays from $U^{235}(n, f)$ and $Pu^{239}(n, f)$ from a few μsec to roughly 50 μsec after fission. The intensities, spectra, and fission isomer yields derived from this experiment, together with results from our previous studies for these two cases of fission, are summarized in this paper.

* Work performed under Contract No. AF29(601)-6837.
† Now at Los Alamos Scientific Laboratory, Los Alamos, N.M.
[1] P. C. Fisher and L. B. Engle, Phys. Rev. **134**, B796 (1964).
[2] F. C. Maienschein, R. W. Peelle, W. Zobel, and T. A. Love, in *Second United Nations Conference on the Peaceful Uses of Atomic Energy, Geneva, 1958* (United Nations, Geneva, 1958), Vol. 15, p. 366.
[3] J. Griffin, Phys. Rev. **134**, B817 (1964).
[4] S. A. E. Johansson, Nucl. Phys. **64**, 147 (1965).
[5] L. Popeko, G. Val'skii, D. Daminker, and G. Petrov, Atomnaya Energiya **19**, 186 (1965) [English transl.: J. Nucl. Energy **20**, 811 (1966)].
[6] R. B. Walton, R. E. Sund, E. Haddad, J. C. Young, and C. W. Cook, Phys. Rev. **134**, B824 (1964).
[7] R. E. Sund and R. B. Walton, Phys. Rev. **146**, 824 (1966).

2. DESCRIPTION OF THE EXPERIMENT

The experimental approach and equipment used for this study were similar to those used previously for $t > 50$ μsec after neutron fission.[7] A schematic drawing of the present setup is provided in Fig. 1. Fast neutrons produced by bombarding a target with a pulse of 30-MeV electrons from the LINAC caused a burst of fissions in a Pu^{239} or U^{235} sample located inside a shield cage. The energy spectrum of these fast neutrons is very similar to that of neutrons from fission. The neutron source strength was monitored by measuring the charge deposited in the target by the beam with a current integrator. Delayed γ rays from the sample were measured in selected time intervals after the beam pulse with a NaI detector which viewed the sample through a 2.8-cm-diam collimating hole in a 2.4-m-thick shield wall. Lithium hydride plugs having a total thickness of 6 gm/cm^2 were placed in the collimator to prevent neutrons from traveling through the collimator to the detector.

Details of the arrangement of the sample, electron target, and the shield cage are shown in Fig. 2. The region seen by the detector, which is defined by the collimation system in the 2.5-m shield wall, is that enclosed by the dashed lines on the drawing. The electron target and sample were surrounded by a box filled with elemental boron which shielded the sample from low-energy neutrons. This shielding was necessary to reduce background γ rays arising from late fissions which were induced by slow neutrons surviving in the time region of interest for the delayed γ-ray measurements. Since the fission cross section is largest at low energies and because each fission yields $\sim$7 prompt γ rays, a relatively small number of slow neutrons could produce a large background. The neutron shielding configuration was optimized by minimizing the yield of capture γ rays from boron and cadmium samples. The addition of bismuth plates at the termination of the collimation system and along the walls of the hole in the boron shield box near the sample location reduced significantly the low-energy

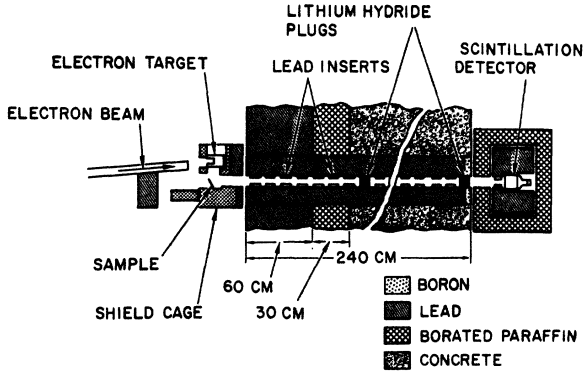

FIG. 1. Schematic drawing of the configuration used for studies of delayed γ rays from neutron fission.

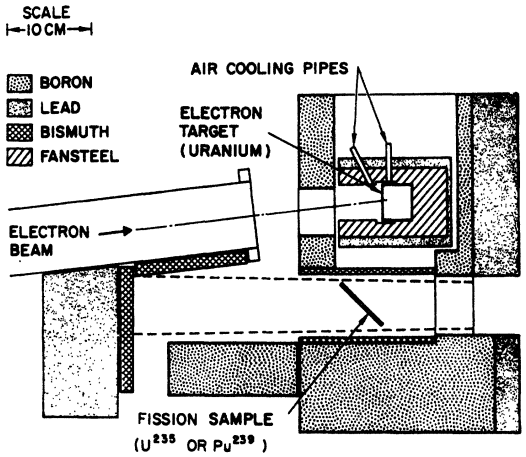

FIG. 2. Details of the sample and source configuration used for measurements of delayed γ rays from neutron fission.

($E_\gamma < 500$ keV) γ-ray background, probably because bismuth does not give rise to isomers with μsec half-lives and because it has a very small neutron-capture cross section.

The electron target used in this experiment consisted of a piece of Al-clad, depleted uranium, approximately six radiation lengths thick, placed inside a 7.5-cm-diam, 12.5-cm-long cylinder of fansteel (a tungsten alloy with a density of 17 g/cm^3) with a hole for the electron beam. This assembly was embedded in lead with outside dimensions 10×10×12.5 cm. A primary consideration in the design of this target was the minimization of the "beam flash," the burst of bremsstrahlung and secondary γ rays generated by the electron beam, which can cause severe overloading of the detector electronics during the beam-pulse duration. The beam flash was also reduced by adding lead at strategic locations along the electron beam tube and between the electron target and the detector.

The U^{235} sample used for these measurements consisted of a stack of foils having an area of 35.5 cm^2 and a total thickness of 2.38 g/cm^2. The sample of Pu had the same area as the U^{235} sample and consisted of four layers of foils. Each layer consisted of Pu, 0.025 cm thick, clad with 0.0076-cm nickel foil and sealed between two 0.038-cm layers of plastic. Samples of aluminum having thicknesses chosen to simulate the scattering and production (by fission) of fast neutrons by the fission foils were used to evaluate backgrounds for these measurements. The same amount of plastic and nickel as contained in the cladding for the Pu foils was included in the background sample for Pu.

The detection system used for this study was a 7.6-cm-diam×7.6-cm-long NaI crystal mounted on an RCA 8054 (10-stage) photomultiplier tube. Signals from the photomultiplier passed through a line driver to a Hamner N301 amplifier, the output of which was fed into a TMC pulse-height analyzer operated in the

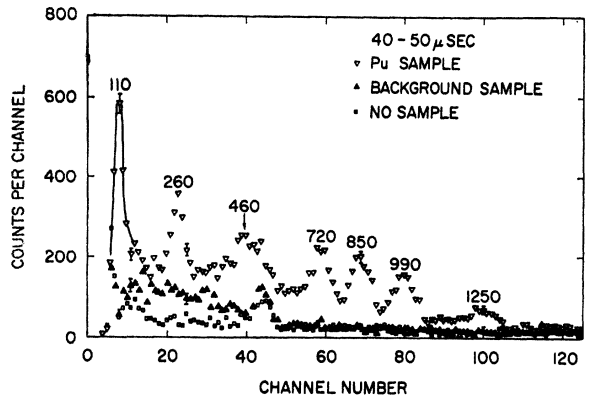

FIG. 3. Pulse-height spectrum of γ rays emitted from the Pu^{239} sample in the interval 40–50 μsec after the beam pulse. For comparison, the spectra taken in the same time interval with the background sample and with no sample, normalized to the same beam monitor reading as that for the Pu data, are also shown. The energies of the prominent photopeaks are given in keV.

coincidence mode. Analysis of pulses occurring within a preselected time interval after the accelerator beam pulse was accomplished by opening the analyzer coincidence gate with amplifier discriminator pulses which had passed through a time gating unit.

Although the general features of the detection system were fairly standard, several special features had to be incorporated to overcome problems inherent to the measurements for $t<50$ μsec. To achieve good timing resolution and minimize the likelihood of pulse pileup, the duration of the pulses was kept less than $\sim$3 μsec by using a small plate-load resistance, 4 kΩ. For the measurements for $t<5$ μsec, the system was modified by adding a pulse-shaping network ahead of the Hamner N301 amplifier to shorten the duration of the pulses to about 2 μsec. The energy resolution at 662 keV was 8% for the system used for $t>5$ μsec and 10% for that used for $t<5$ μsec. Because the beam flash was very severe, even after the extensive improvements in the shielding, an off-gating unit, which effectively biased the photomultiplier tube off during the accelerator beam pulse, was developed for this experiment. The biasing was obtained by placing simultaneously 150-V pulses having opposite polarities on the first and third dynodes of the photomultiplier tube. A signal suppression factor of about 100 was obtained with this system.

The detection system was calibrated using the following sources of γ rays: Ba^{133} (81, 302, 355 keV), Co^{57} (122 keV), Na^{22} [511, 1275, 1786 keV (sum peak)], Cs^{137} (662 keV), Mn^{54} (835 keV), and Co^{60} [1170, 1330, 2500 keV (sum peak)]. The amplitudes of the photpeaks produced by these sources showed that the system used for measurements for $t>5$ μsec covered with approximate linearity the range of energies between 80 and 2500 keV and had a saturation level of $\sim$3500 keV. The modified detection system that was used for $t<5$ μsec covered with approximate linearity the range of energies between 80 and 2000 keV and saturated at $\sim$2500 keV.

3. RESULTS

A. Experimental Data

The data for each time interval after the beam pulse consisted of a pulse-height distribution taken with the fission sample in place, and, for evaluation of the time-dependent background, pulse-height distributions taken with no sample and with a background sample. The long-term activity of the fission sample, i.e., the natural activity and the activity from past beam pulses, was measured in a time interval just preceding the accelerator pulse. Measurements of the ambient background, which is the background present when the accelerator was shut off and the sample removed, were made before and after each run with the accelerator.

The rate of accumulation of delayed γ-ray data was governed by the beam repetition rate and by the instantaneous counting rate which the detector electronics and pulse-height analyzer could handle. The beam repetition rate had to be limited to keep the long-term activity of the fission sample at a level appreciably smaller than that of the delayed γ rays produced by a single beam pulse. For the repetition rates used for this study, which ranged from 30 pps (pulses per second) for the intervals later than 30 μsec after the beam pulse to 120 pps for the earliest interval investigated, the long-term activity was usually less than 10% of the delayed-γ-ray intensity. The accelerator beam intensity was adjusted to give instantaneous counting rates less than 0.015 counts/μsec, so that the likelihood of pulse pileup was negligible and the analyzer counting losses were always less than about 8% and could be accounted for accurately. With these operating conditions the time required to obtain a pulse-height distribution of the γ rays emitted from the fission sample in a single time interval after the beam pulse was typically 1.5 to 3 h.

Pulse-height distributions of the γ rays emitted after Pu(n, f) were measured for the following time intervals: 2–3 μsec, 3–5 μsec, 5–7.5 μsec, 7.5–10 μsec, 10–15 μsec, 20–30 μsec, 30–40 μsec, 40–50 μsec, and 70–80 μsec. Similar data were taken for $U^{235}(n, f)$ in two time intervals, 5–7.5 μsec and 40–50 μsec.

The significant features of these data may be seen in the examples given in Figs. 3 and 4, which are pulse-height distributions for Pu in the intervals 40–50 μsec and 5–7.5 μsec, respectively. Only the portion of the pulse-height scale which contains all of the photopeaks observed in this study is displayed in the figures. As determined from measurements with γ-ray sources, the lowest channel for which no counts were rejected by the discriminator is channel 6 ($E_\gamma \sim 70$ keV). The Pu data have been corrected for counting losses and for the ambient background and the long-term

activity of the sample; however, they were not corrected for time-dependent backgrounds. The error bars in these figures indicate only the statistical uncertainties of the data. In the pulse-height distribution for Pu in the interval 40–50 μsec, photopeaks corresponding to the six γ rays with energies 260, 460, 720, 850, 990, and 1250 keV, which had been observed in our previous investigation,[7] are apparent. The γ-ray energies given here differ slightly from the values determined previously and are believed to be more accurate because of improvements made in the calibration and monitoring of the detection system. The photopeak at about 110 keV was not seen in the previous study because the lower limit of the γ-ray energy range covered in that experiment was 140 keV. In the data for Pu in the interval from 5 to 7.5 μsec, new prominent γ rays at about 110, 205, 390, and 1330 keV are apparent. The six higher-energy γ rays which appeared clearly in the later time interval are less evident in the 5–7.5-μsec data because at the earlier times their intensities are much less than those of the new γ rays.

Data obtained with no sample and with the background sample during the intervals 40–50 μsec and 5–7.5 μsec have been included for comparison in Figs. 3 and 4. For both time intervals shown, it is evident that the intensity with the background sample was about the same as that with no sample for pulse heights greater than channel 50 ($\sim$600 keV) but was larger over most of the lower range. Some structure in the data for the background sample and for no sample is evident near channel 43 for the 40–50-μsec interval and near channels 43 and 11 for the 5–7.5-μsec data; however, for both time intervals the difference between the background sample data and the no-sample data shows no significant structure, indicating that neutrons or γ rays scattered by the sample do not give rise to any strong photopeaks.

In attempts to correct the delayed γ-ray data for the time-dependent background caused by the scattering and production (by fission) of fast neutrons, we found that subtraction of the data obtained with the background sample from that with the fission sample produced a correction which was obviously too large; i.e., physically unrealistic minima appeared between the low-energy photopeaks in the net pulse-height distributions. This could result because (1) the number of neutrons scattered from the background sample did not match that from the fission sample, and (2) a significant number of the time-dependent background γ-rays originated in the area of the collimation system beyond the sample as viewed by the detector, and were, therefore, attenuated more severely by the fission sample than by the background sample. The latter effect seems to be the more significant because the "oversubtraction" is greater for the lower-energy γ rays.

As an alternative procedure for applying approximate

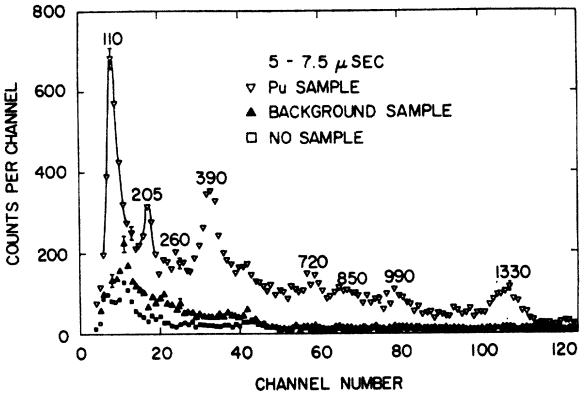

FIG. 4. Pulse-height spectrum of γ rays emitted from the Pu^{239} sample in the interval 5–7.5 μsec after the beam pulse. For comparison, the spectra taken in the same time interval with the background sample and with no sample, normalized to the same beam monitor reading as that for the Pu data, are also shown. The energies of the prominent photopeaks are given in keV.

corrections for time-dependent backgrounds, we chose to subtract the data obtained with no sample from the data taken with the fission sample, being careful to note any artificial features generated by this subtraction which might significantly change the areas under the photopeaks of the prominent fission-delayed γ rays. Since the areas under the peaks near channels 43 and 15 in the background-sample data are approximately the same as the corresponding areas in the no-sample data, no distortions of the delayed γ-ray photopeaks should occur in these regions by subtracting the no-sample data from the fission-sample data. Furthermore, the subtractions resulted in a clearer photopeak for the 460-keV γ rays which had been observed in the previous study for longer time delays.[7] For the channels below number seven in the pulse-height distributions, subtraction of the no-sample data still gave an oversubtraction for some of the time intervals and a consequent uncertainty in the 110-keV photopeak area.

Figures 5 and 6 display the differences between the fission-sample data and the data taken with no sample for four representative delay time intervals. Before the subtractions were performed, the Pu data and the no-sample data were corrected for counting losses and ambient backgrounds, and, in addition, the Pu data were corrected for the background due to long-term activity of the fission sample. The Pu data in the region of the 110-keV photopeak have also been displayed on the same plots to demonstrate the uncertainties caused by the estimate of the time-dependent background. The statistical uncertainties of the data are indicated by the error bars on a few representative points in the spectra. Comparisons of the intensities of the photopeaks in the different time intervals may be made by weighting the data for each interval by the inverse of the factor $Q\Delta t$, which is given on each plot and is proportional to the product of the

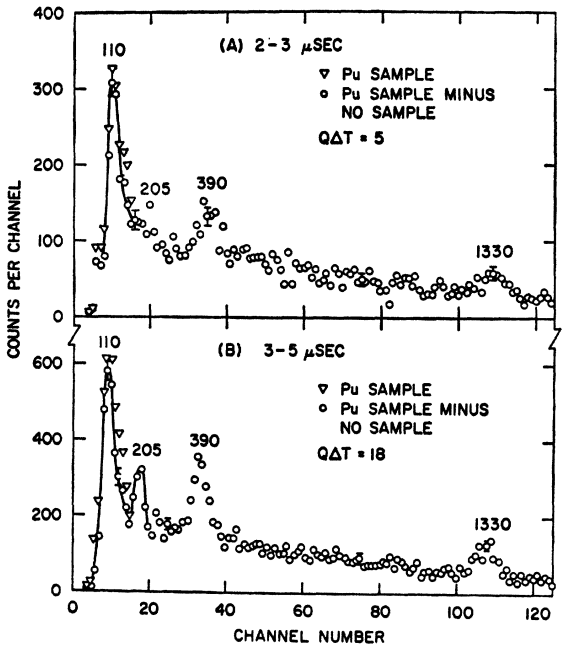

FIG. 5. (A) Difference between the pulse-height spectrum obtained in the interval 2–3 μsec with the Pu sample and that with no sample. The data for the Pu sample are also shown in the region of the 110-keV peak. The energies of the prominent photopeaks are given in keV. (B) Same as (A) except in the interval 3–5 μsec.

integrated electron beam current of the run with the Pu sample and the width of the time gate interval.

The data for U^{235} in the two time intervals 5–7.5 μsec and 40–50 μsec, which are not shown, are quite similar to the data displayed for Pu^{239}. The fact that the same γ rays were observed in these two intervals for both Pu and U^{235} is a positive indication that these γ rays arise from fission product isomers rather than some other neutron reaction with one or the other fissionable isotope. Since the decay periods for the new short-period γ rays could be derived from the Pu^{239} data, the measurements for U^{235} in only two time intervals were sufficient to specify the yields of the new γ rays relative to the six γ rays studied previously.

An additional set of data for one time interval (10–15 μsec) was taken using a single layer of Pu foil (one-quarter of the thickness of the sample normally used) in order to reduce the self-absorption of low-energy γ rays and hence permit a check of their intensities relative to those of the γ rays with higher energies. This measurement was especially important for the interpretation of the data between channels 5 and 15 because these channels bracket the K absorption edge of Pu (and U^{235}). In particular, it is possible that the peak in the pulse-height distributions near channel 10 was caused by a continuous spectrum of low-energy background γ rays that was distorted by the sharply varying γ-ray absorption in the energy region of the K edge (~120 keV). A possible continuous background of γ rays could be the prompt γ rays from late fissions. Comparisons of the data for the thick and thin Pu samples, corrected for γ-ray transmission, are consistent with the assumption that this peak is a real photopeak resulting from the detection of one or more prominent delayed γ rays; however, because of the experimental errors, a definite conclusion cannot be reached on the basis of these data.

B. Data Analysis

In specifying the yields and time dependence of the delayed γ rays observed in this study, we considered only those γ rays which produced prominent photopeaks. From the data shown in Figs. 5 and 6, it is evident that most of the counts between photopeaks can be accounted for by the Compton tails of the pulse-height spectra produced by the prominent γ rays; however, it is possible that some of these counts could be due to unresolved γ rays from low-yield fission isomers. In addition, for all but the latest time interval (70–80 μsec), a low-level, slowly varying distribution of counts extended far beyond the pulse height of the highest photopeak (1.33 MeV), indicating that a portion of the pulse-height spectra may be due to either the continuous spectrum of prompt γ rays from

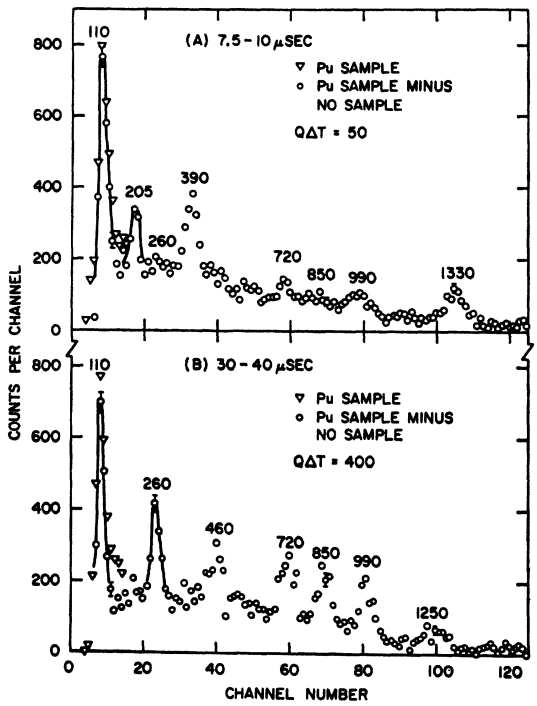

FIG. 6. (A) Difference between the pulse-height spectrum obtained in the interval 7.5–10 μsec with the Pu sample and that with no sample. The data for the Pu sample are also shown in the region of the 110-keV peak. The energies of the prominent photopeaks are given in keV. (B) Same as (A) except in the interval 30–40 μsec.

"late" fissions or so some other cause which could not be directly isolated in this experiment.

The half-life plots for the new γ rays with energies of 205, 390, and 1330 keV, which were derived from the Pu pulse-height spectra, are presented in Fig. 7. The relative counting rate for a particular γ ray was determined from the areas enclosed by its photopeak in the spectra for the various time intervals. The photopeak area for each interval was normalized by dividing it by the value of $Q\Delta t$ for that interval, and the midpoint times of the Δt intervals were corrected for the approximate half-life of the transition. For convenience in plotting, the data for each of the three γ rays were multiplied by an arbitrary constant and then plotted as shown in Fig. 7. The error shown for each datum point consists of the statistical uncertainty in the sum of the counts in the channels spanning the photopeak plus an uncertainty in the estimate of the counts in the continuous "base-line" spectrum on which the photopeak was superimposed. The latter uncertainty was usually a great deal larger than the statistical uncertainty in the photopeak sum. Least-squares fits to these data were performed to determine the half-lives for the transitions and the relative intensities of the photopeaks as a function of time after fission. The resulting fits to the data are indicated by the lines in the figure.

The decay of the 110-keV photopeak observed in the Pu data could not be fitted with a single exponential; hence, we assumed that two unresolved γ rays resulting from the decay of two isomers with appreciably

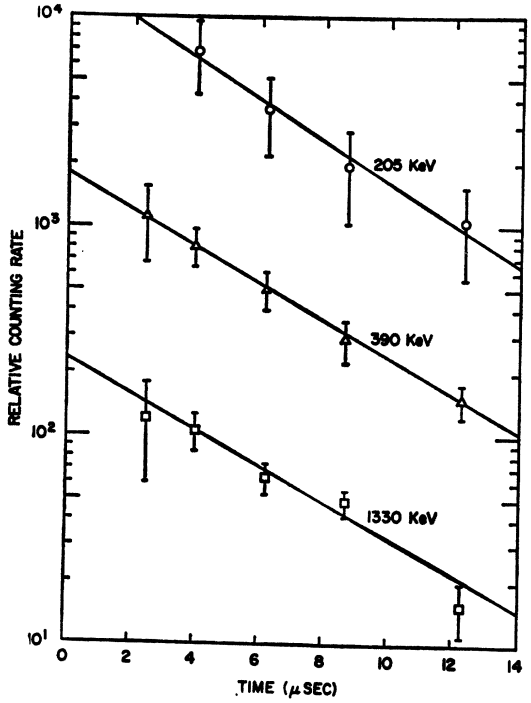

FIG. 7. Half-life plots for the 205-, 390-, and 1330-keV γ rays observed following $Pu^{239}(n, f)$. The lines show the least-squares fits to the data with single exponentials.

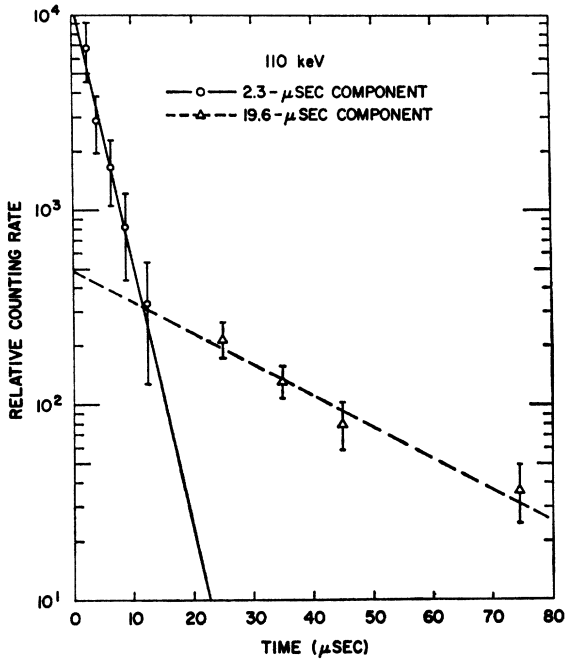

FIG. 8. Synthesis of the data for the relative intensity of the 110-keV photopeak into two exponential components. Experimental data points for each of the components, together with lines representing least-squares fits to the data, are shown.

different half-lives contributed to the photopeak. The data were fitted approximately with two exponentials, and then an iterative procedure was used to obtain the least-squares fits to the data with two exponentials. Figure 8 shows the experimental data points for each of the components resulting from this synthesis, together with the final least-squares fits that are indicated by the straight lines.

The half-life plots for the 720-keV and 990-keV γ rays, which result from the decay of a single isomer (Ref. 7), are shown in Fig. 9. The average of the half-lives derived from the present data for these two γ rays is 26.7 ± 3.0 μsec, which is in satisfactory agreement with the previously determined value of 32.0 ± 3.5 μsec. On the basis of the number of data points and the time region which these points covered, we believe that the new half-life determination is the better and have used the new value to revise the absolute yields derived in the previous work. Although the data obtained in the present study for the γ rays with energies 260, 460, 850, and 1250 keV did not cover a time range sufficiently long to warrant new half-life determinations, the plots of their intensities as a function of time are consistent with the half-lives determined previously.[7]

In the next step of the data analysis, the relative intensities of all the $Pu(n, f)$ delayed γ rays were extrapolated to $t=0$ with the appropriate exponentials and were then corrected for the photopeak-to-total ratios, the efficiency of the detector, and the attenuation of the γ rays by the Pu sample and the LiH plugs.

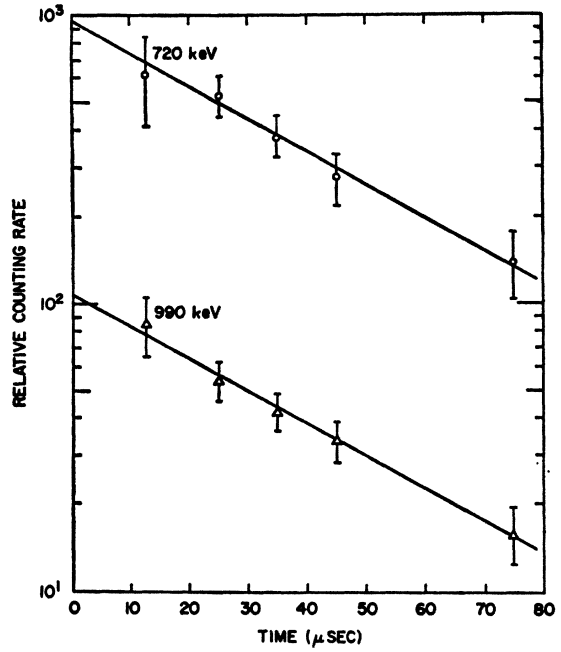

FIG. 9. Half-life plots for the 720- and 990-keV γ rays observed following $Pu^{239}(n, f)$. The lines show the least-squares fits to the data with single exponentials.

Measurements of the attenuation of the LiH plugs as a function of energy from 80 to 1276 keV were performed in this study, and the results showed that the attenuation factors for the LiH used in the previous study were in error by a small amount for energies below 400 keV. The only γ-ray intensity affected by this error was that for the 260-keV γ ray, being 10% smaller than the previously reported value.[7] Since the correction of the intensity of this γ ray brings it into even better agreement with the intensity of the 850-keV γ ray, the original conclusion that these two γ rays result from the cascade decay of one isomer still holds; however, the yield of this isomer, which was computed from the average of the intensities of these γ rays, is lowered by 5%.

Table I gives the corrected relative intensities and half-lives derived for the new γ rays observed for $Pu(n, f)$ and $U^{235}(n, f)$. The relative intensities of the delayed γ rays from $U^{235}(n, f)$ were extrapolated to $t=0$ using the half-lives derived from the Pu data and subsequently were corrected for the γ-ray attenuation and the detector characteristics.

TABLE I. Energies, half-lives, and relative intensities at $t=0$ of the new delayed γ rays from $Pu^{239}(n, f)$ and $U^{235}(n, f)$.

Energy (keV)	Half-life (μsec)	Relative intensity at $t=0$ $Pu^{239}(n,f)$	$U^{235}(n,f)$
(110)	(2.3±0.5)	(720±340)	(740±400)
(110)	(19.6±4.6)	(30±13)	(32±16)
205	3.1±1.0	155±90	86±70
390	3.4±0.5	154±40	73±28
1330	3.6±0.7	153±40	71±32

The close agreement of the half-lives and relative intensities for the 205-, 390-, and 1330-keV γ rays for both $Pu^{239}(n, f)$ and $U^{235}(n, f)$ suggests that these γ rays result from the cascade decay of a single isomer, provided that the internal conversion coefficients for these transitions are small. Upper limits of the internal conversion coefficients for these transitions were obtained by the procedure described in Ref. 7. Since the emission sequence of the proposed cascade γ rays is unknown, we assumed that any of the three could be the one which deexcites the isomeric state. Thus for each γ ray, the γ-ray transition probabilities for all possible multipole orders were computed using the measured half-life and theoretical values of the internal conversion coefficient[8] for the range of atomic numbers covered by fission fragments. These transition probabilities were then compared with a compilation of experimental results[9] for γ-ray transitions of known energy and multipolarity to obtain the possible multipole orders for the γ ray in question. The values of α_{max}, the largest internal conversion coefficient consistent with the possible multipolarities, were obtained from tabulations for an atomic number $Z=59$, which is the highest fragment Z with yield sufficient to explain the observed γ-ray intensities. (See below.) Results for the possible multipole orders and values of α_{max} are presented in Table II. The values of α_{max} for the 390- and 1330-keV transitions are sufficiently small that either of these γ rays could deexcite the isomeric state. The internal conversion coefficient for a 205-keV, $E2$ transition for $Z=59$ is 0.17, which is small enough to be consistent with a cascade starting with the emission of the 205-keV γ ray. However, in the case of a cascade starting with a 205-keV, $M2$ transition, the emitting fragment would probably be in

TABLE II. Most probable multipolarities and corresponding maximum internal conversion coefficients for the 205-, 390-, and 1330-keV transitions, with the assumption that each of the γ rays deexcites an isomeric state.

γ-ray energy (keV)	Most probable multipolarities	α_{max}
205	$E2, M2$	1.0
390	$E2, M2$	0.1
1330	$E3, M3$	0.007

[8] L. A. Sliv and I. M. Band, in *Alpha-, Beta-, and Gamma-Ray Spectroscopy*, edited by K. Siegbahn (North-Holland Publishing Co., Amsterdam, 1965), Vol. 2, Appendix 5.

[9] E. Segrè, *Experimental Nuclear Physics* (John Wiley & Sons, Inc., New York, 1959), Vol. 3, Part X.7; J. Lindskog, T. Sundstrom, and P. Sparrman, in *Alpha-, Beta-, and Gamma-Ray Spectroscopy*, edited by K. Siegbahn (North-Holland Publishing Co., Amsterdam, 1965), Vol. 2, Appendix 3.

TABLE III. Energies, half-lives, and absolute intensities of isomeric γ rays at $t=0$ for $Pu^{239}(n,f)$ and $U^{235}(n,f)$.

Energy (keV)	Half-life (μsec)	Absolute intensity after $Pu^{239}(n,f)$ (photons/fission-sec)	Absolute intensity after $U^{235}(n,f)$ (photons/fission-sec)
(110)	(2.3±0.5)	(12 400±6000)	(12 700±7100)
(110)	(19.6±4.6)	(520±230)	(540±280)
1330, 390, 205	3.4±0.4	2660±590	1280±410
850, 260	54.0±2.5	93±10	109±13
1250, 460	80±3	39.6±3.2	27.4±4.4
990, 720	26.7±3.0	190±35	117±30

the lower bump of the mass-yield curve; if it were in the upper bump, the internal conversion coefficient would be large enough to make the total transition intensities disagree by a significant amount. From these arguments it is evident that the 205-, 390-, and 1330-keV γ rays probably do result from the cascade decay of a single isomer.

The corrected relative intensities of the new γ rays (see Table I) were converted to absolute intensities by means of a normalization factor derived from the relative intensities of the 260-, 460-, 720-, 850-, 990-, and 1250-keV γ rays and their known absolute intensities. For this normalization we have assumed that the intensities of the delayed γ rays from fission by thermal neutrons, as used in the previous work,[7] are the same as those from fission by the fast neutrons used in the present study. The errors caused by this assumption are probably small because the average charge distribution of the fragments is shifted little by a change of $\sim$2 MeV in neutron bombarding energy. The resulting intensities, together with the intensities of the six γ rays studied previously,[7] are presented in Table III. The data from the previous study have been corrected for the improved LiH attenuation factors and for the improved half-life determination. γ rays originating from the same isomer have been grouped together, and the common intensity and common half-life listed for them represent the averages of the data for the individual γ rays; the uncertainties given in Table III were derived from those for the individual γ rays. For all γ rays except the two with energies of 110 keV, the errors shown in Table III were obtained from the uncertainties in the pulse-height distribution data. In the case of the 110-keV γ rays, the uncertainty in the attenuation by the sample was significant and has been included in the errors shown. All of the γ-ray intensities have a common uncertainty of $\pm$20%, not included in Table III, which is due to the normalization of the previous data[7] in the plateau region to the absolute results obtained from the work of Fisher and Engle[1] and of Griffin.[3] Furthermore, according to the experimental results of Seyfarth,[10] an error exists in the β-decay data which Griffin used to establish some of the parameters in his theory. However, the error reflected in Griffin's γ-ray intensities in the plateau region is probably less than 15%, since Griffin's γ-ray intensities fit the experimental data of Fisher and Engle for times greater than 0.35 sec after fission, and the shapes of Griffin's β-decay curves for times less than 0.35 sec agree within about 15% with the shapes obtained by Seyfarth. It should be noted that the magnitude of the β-decay curve changes by only about 20% or less for times less than 0.35 sec.[3,10]

As indicated by the parentheses enclosing the data given in Tables I and III, the results for the two 110-keV γ rays are regarded as only probable because of the uncertainties in the interpretation and reduction of the data for the 110-keV photopeak. Because the absolute intensity of the 2.3-μsec, 110-keV γ ray corresponds approximately to the largest independent fission product yield (see Sec. 4), the internal conversion coefficient for this transition would have to be small. This consideration, as well as energy and half-life considerations, limits the most probable multipolarity to $E1$ or possibly to $M1$, provided that in the latter case the fragment is in the lower bump of the mass-yield curve. The energy and half-life for the tentative 110-keV, 19.6-μsec transition indicate that the most probable multipolarities are $E2$ or $M2$. For an $E2$ transition the internal conversion coefficient varies between 0.7 and 1.5 for the range of Z allowed by the yield. These values for the internal conversion coefficient are consistent with the observed yield (see

TABLE IV. Summary of the half-lives, energies of cascade γ rays, and yields of isomers produced by $Pu^{239}(n,f)$ and $U^{235}(n,f)$.

Isomer half-life (μsec)	Energies of cascade γ rays (keV)	Fission yield[a] (% per fission) $Pu^{239}(n,f)$	$U^{235}(n,f)$
3.4±0.4	1330, 390, 205	1.30±0.30	0.63±0.20
26.7±3.0	990, 720	0.73±0.15	0.45±0.12
54.0±2.5	850, 260	0.72±0.06	0.85±0.07
80±3	1250, 460	0.46±0.03	0.32±0.05
(2.3±0.5)[b]	(110)	($\sim$4.0±2.0)	($\sim$4.1±2.2)
(19.6±4.6)[c]	(110)	(>1.5±0.7)	(>1.5±0.8)

[a] All isomer yields have a common uncertainty of $\pm$20%, not included in the table, which results from the normalization of the delayed γ-ray intensities. (See text and Ref. 7.)

[b] The yield given in the table for this proposed isomer is essentially equal to the maximum independent fission yield and was computed assuming a negligible internal conversion coefficient. The possible multipolarities for this transition are $E1$ and $M1$, the latter being less likely.

[c] The γ-ray yield for this proposed isomer is 1.5% per fission. The internal conversion coefficients corresponding to the most probable multipole orders ($E2$, $M2$) for this transition would require that the total yield of the isomer be between $\sim$1.7 times this γ-ray yield and the largest possible fission fragment yield.

[10] H. Seyfarth, Nucleonik 10, 193 (1967).

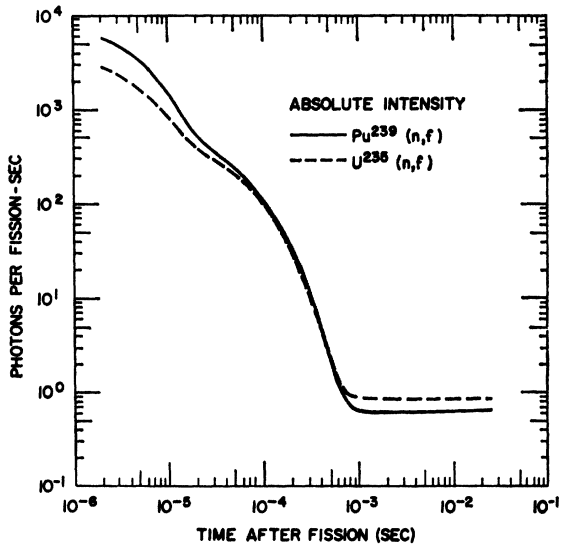

FIG. 10. Absolute intensities of γ rays (photons/fission-sec) with $E_\gamma > 140$ keV as a function of time after $U^{235}(n, f)$ and $Pu^{239}(n, f)$.

Sec. 4) and the maximum possible fission fragment yield. Because of yield considerations, an $M2$ transition would only by possible for Z less than about 40.

4. CONCLUSIONS

The absolute yields of the isomers from $Pu^{239}(n, f)$ and $U^{235}(n, f)$ which emitted the delayed γ rays observed in this study and in the previous measurements for $t > 50$ μsec are presented in Table IV. The yields for the four cascades listed in the table were calculated with the assumption that the internal conversion coefficients are small. Considerations of the possible multipolarities consistent with the observed γ-ray energies and half-lives support this assumption. The effects of the internal conversion coefficients on the yields for the two proposed 110-keV isomers are listed in the footnotes in Table IV. Because the uncertainties in the data for the half-lives and intensities of the 1330-, 390-, and 205-keV γ rays were relatively large, the assignment of these transitions to the cascade decay of a single isomer is somewhat less certain than the other cascade assignments. The conclusions for the two 110-keV γ rays must be regarded as tentative (as indicated by the parentheses) because the possibility that the 110-keV photopeak was produced by the

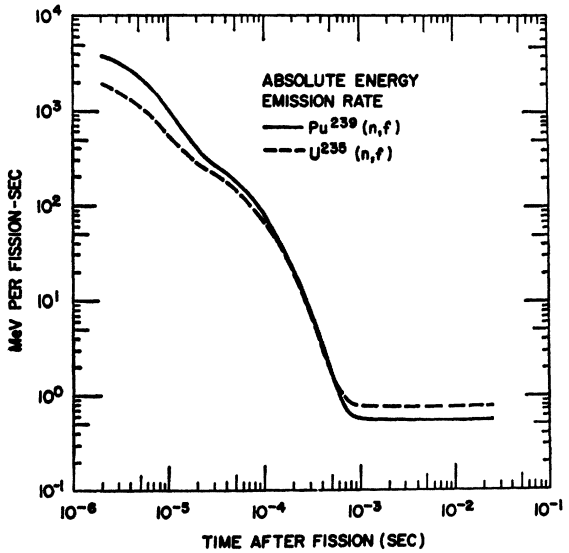

FIG. 11. Absolute energy emission rates (MeV/fission-sec) for $E_\gamma > 140$ keV as a function of time after $U^{235}(n, f)$ and $Pu^{239}(n, f)$.

TABLE V. Absolute γ-ray intensities and energy emission rates as a function of time after neutron fission for $E_\gamma > 140$ keV.

Time (sec)	Absolute intensity (photons/fission-sec) Pu^{239}	U^{235}	Absolute energy emission rate (MeV/fission-sec) Pu^{239}	U^{235}
0	8610	4355	5607	2837
2×10^{-6}	5909	2965	3869	1943
4×10^{-6}	4147	2066	2735	1364
6×10^{-6}	2898	1482	1931	987
8×10^{-6}	2095	1100	1411	740
1×10^{-5}	1563	848	1067	576
1.2×10^{-5}	1175	681	814	468
1.4×10^{-5}	919	569	647	394
1.6×10^{-5}	747	493	534	344
1.8×10^{-5}	632	439	458	308
2×10^{-5}	552	401	404	282
4×10^{-5}	305	253	226	177
6×10^{-5}	214	184	157	126
8×10^{-5}	155	136	112	92
1×10^{-4}	114	103	83	70
1.5×10^{-4}	57	53	41	37
2×10^{-4}	32	29	23	21
3×10^{-4}	11.3	10.9	8.5	7.4
4×10^{-4}	4.6	4.3	3.7	3.3
5×10^{-4}	2.2	2.2	1.77	1.78
6×10^{-4}	1.28	1.41	1.05	1.18
7×10^{-4}	0.90	1.08	0.76	0.95
8×10^{-4}	0.74	0.95	0.64	0.85
1×10^{-3}	0.66	0.87	0.57	0.79
1.2×10^{-3}	0.64	0.85	0.56	0.78
2.5×10^{-2}	0.64	0.85	0.56	0.78

transmission of background γ rays through the thick samples could not be absolutely ruled out. The yield of the proposed 2.3-μsec isomer is unusually high, but is consistent with the larger independent yields calculated for fission products. From the results given in Table IV, it is apparent that the individual isomer yields from $Pu^{239}(n, f)$ and $U^{235}(n, f)$ are usually significantly different, and the largest difference, a factor of about 2, occurs for the 3.4-μsec isomer. Furthermore, comparison of these yields with abundances of fission products given in the literature[11] indicates that the isomers fall within the approximate ranges of atomic number and mass (Z, A) from (33, 84) to (43, 105) and from (50, 129) to (59, 150), i.e., the regions containing the peaks in the mass-yield curve.[7]

There may be additional γ rays emitted after fission, which were missed in these studies because either their intensities fell below the minimum sensitivity of the detection apparatus or their energies were outside the region spanned in these experiments; however, the dominant features of the γ-ray emission from fission beyond 2 μsec are specified by the results of the present study and previous work.[1-3,6,7] The total γ-ray intensities (in photons/fission-sec) and the total γ-ray energy emission rates (in MeV/fission-sec) from $Pu^{239}(n, f)$ and $U^{235}(n, f)$ have been computed as a function of time over the interval from 2 μsec to the plateau region using the data given above and previous results. The 110-keV γ rays were not included because of their uncertainty and because the lower limit of the γ-ray energies studied previously was 140 keV. The results of these calculations are displayed in Figs. 10 and 11 and are also listed in Table V.

[11] R. C. Bolles and N. E. Ballou, U.S. Naval Radiological Defense Laboratory, San Francisco, Report No. 456, 1956 (unpublished); L. R. Bunney, E. M. Scadder, J. O. Abriam, and N. E. Ballou, in *Second United Nations Conference on the Peaceful Uses of Atomic Energy, Geneva, 1958* (United Nations, Geneva, 1958), Vol. 15, p. 444; M. P. Anikina, P. M. Aron, V. K. Gorshkov, R. N. Ivanov, L. M. Krizhansky, G. M. Kukaradze, A. N. Murin, I. A. Reformatsky, and B. V. Ershler, in *Second United Nations Conference on the Peaceful Uses of Atomic Energy, Geneva, 1958* (United Nations, Geneva, 1958), p. 446.

ACKNOWLEDGMENTS

The authors are grateful for the helpful advice given by Dr. J. R. Beyster and many other persons at the Gulf General Atomic Accelerator Physics Department during the course of these measurements. Particular thanks are due to P. Phelps, J. Riggs, and P. Heid for developing the electronics for this experiment, A. Dolinski for assembling the experimental equipment and taking data, and M. Baker for helping with data acquisition and analysis.

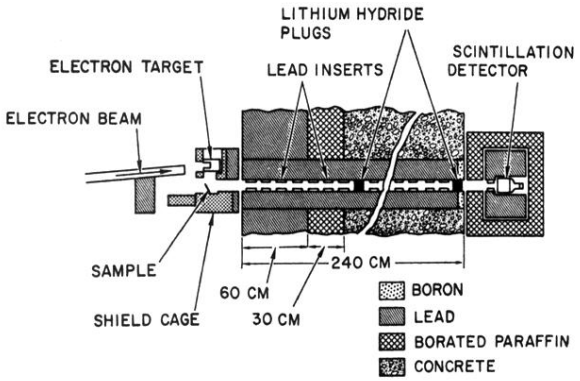

FIG. 1. Schematic drawing of the configuration used for studies of delayed γ rays from neutron fission.

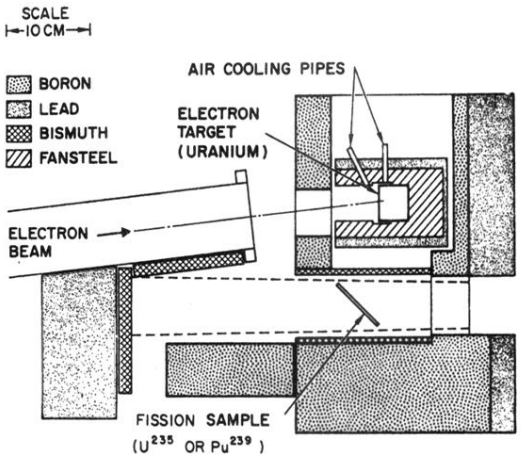

FIG. 2. Details of the sample and source configuration used for measurements of delayed γ rays from neutron fission.